A Wideband Slotted Bow-Tie Antenna With Reconfigurable CPW-to-Slotline Transition for Pattern Diversity

Sung-Jung Wu and Tzyh-Ghuang Ma, *Member, IEEE*

***Abstract*—We propose a slotted bow-tie antenna with pattern reconfigurability. The antenna consists of a coplanar waveguide (CPW) input, a pair of reconfigurable CPW-to-slotline transitions, a pair of Vivaldi-shaped radiating tapered slots, and four PIN diodes for reconfigurability. With suitable arrangement of the bias network, the proposed antenna demonstrates reconfigurable radiation patterns in the frequency range from 3.5 to 6.5 GHz in three states: a broadside radiation with fairly omnidirectional pattern and two end-fire radiations whose mainbeams are directed to exactly opposite directions. The proposed antenna is investigated comprehensively with the help of the radiation patterns in the two principal cuts and also the antenna gain responses versus frequencies. The simulation and measurement results reveal fairly good agreement and hence sustain the reconfigurability of the proposed design.**

***Index Terms*—Coplanar waveguides, PIN diodes, reconfigurable antennas, slotline transitions, wideband antennas.**

I. Introduction

In RECENT years, reconfigurable antennas have received significant attentions in the field of wireless communications. These antennas are capable of achieving selectivities in the operating frequencies, polarizations, radiation patterns, as well as gains. In modern wireless systems, data streams over the air interface are always propagated in multipath-rich environment and interfered severely by the reflections or diffractions from buildings, landforms or near-by objects. In addition, systems operated in adjacent frequency channels may give rise to significant performance degradation as well. To tackle these problems, diversity techniques, including spatial diversity, angle (pattern) diversity, temporal diversity, as well as polarization diversity, etc., are commonly used in wireless communications to increase the signal-to-noise (SNR) ratio and hence the overall performance. A straightforward way to achieve diversity capability in a wireless system is to use an antenna with reconfigurability which may alternatively be switched between several predetermined states for diversity purpose.

Three major categories of reconfigurable antennas are commonly discussed in the antenna community. Antennas with frequency reconfigurability play a crucial role in integrated systems which aim at using a single multifunctional antenna for several services [1]–[3]. The radiation patterns of these antennas, on the other hand, remain principally unchanged as the operating frequency switches. The second sort of reconfigurable antenna demonstrates pattern reconfigurability over the frequency band of interest [4]–[6]. Such antennas are capable of steering their radiation beams or nulls in several predefined reception directions, and therefore fulfill the requirements of angle diversity in a given operation frequency band. Yet another type of reconfigurable antenna with polarization-agile characteristics has been reported in [7]–[9]. Such antennas are commonly designed on the base of microstrip patch antennas so as to switch the antenna polarization states between right-hand circular polarization (RHCP), left-hand circular polarization (LHCP), and linear polarizations (LPs). Antennas simultaneously possessing two of the abovementioned three reconfigurabilities have also been reported in [10], [11].

Reconfigurable antennas are commonly designed by incorporating switching PIN diodes on the antenna topology. With suitably arranged forward- or reverse-biased PIN diodes by dc bias network, the antenna topology can be rearranged in a systematic way for reconfigurability. RF-MEMS switches are also commonly used in reconfigurable antennas [1], [5], [12], [13]. In addition, frequency and pattern reconfigurable antennas with fractal topologies [14], [15] as well as polarization-agile antenna with mutually coupled oscillating doublers [16] have also been found in the literatures.

In this paper, we propose a slotted bow-tie antenna with a new reconfigurable CPW-to-slotline transition. This antenna consists of four parts, i.e., a coplanar waveguide (CPW) input, two CPW-to-slotline transitions, a pair of Vivaldi-shaped tapered slots as the radiator, and four PIN diodes for reconfigurability. Depending on the dc biased states of the PIN diodes, the proposed antenna can be fed by one of the three feeding configurations, namely the CPW feeding mode, the right-hand slot feeding mode, and the left-hand slot feeding mode. With the newly proposed reconfigurable transition, the antenna demonstrates alternatively switchable radiation patterns between a broadside radiation with fairly omnidirectional

Manuscript received April 11, 2007; revised October 2, 2007. This work was supported by the National Science Council, R.O.C., under Grants 95-2221-E-011-021 and 96-2221-E-011-007.

S.-J. Wu was with the Department of Electrical Engineering, National Taiwan University of Science and Technology, Taipei 10607, Taiwan, R.O.C. He is now with National Chiao Tung University, Hsinchu, Taiwan, R.O.C., and also with Sunplus Technology Co., Ltd., Hsinchu 300, Taiwan, R.O.C.

T.-G. Ma is with the Department of Electrical Engineering, National Taiwan University of Science and Technology, Taipei 10607, Taiwan, R.O.C. (e-mail: tgma@ee.ntust.edu.tw).

Color versions of one or more of the figures in this paper are available online at http://ieeexplore.ieee.org.

Digital Object Identifier 10.1109/TAP.2007.915454

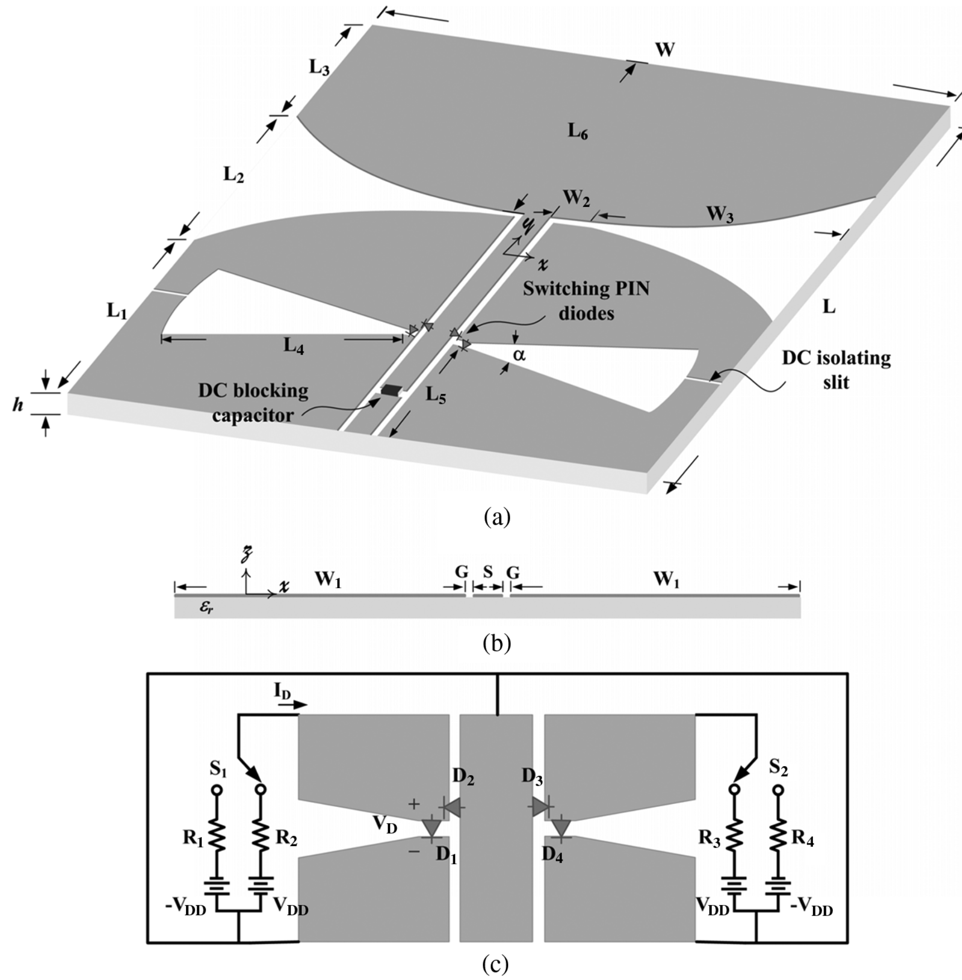

Fig. 1. Configuration of the proposed antenna. (a) Three-dimensional view. (b) Cross-sectional view. (c) PIN diodes arrangement and the associated dc bias network.

pattern and two end-fire radiations whose mainbeams point to exactly opposite directions in the operating range from 3.5 to 6.5 GHz. The organization of the paper is as follows. The antenna configuration and the design concept for pattern reconfigurability are first discussed in Section II. The simulated and measured antenna radiation patterns operated in all three feeding schemes are illustrated in Section III. The gain responses versus frequencies in four specific directions are then addressed along with various discussions. Finally, the paper is concluded with a brief summary in Section IV.

II. Antenna Configuration and Design Concept

Shown in Fig. 1 is the proposed pattern reconfigurable slotted bow-tie antenna. The antenna, which is composed of a CPW input, two CPW-to-slotline transitions, a pair of Vivaldi-shaped tapered slotlines, and four switching PIN diodes along with the associated bias network, lies in the xy-plane with its normal direction parallel to the z-axis. The signal is fed to the CPW input line via a SMA connector. The input CPW, which is cascaded by a pair of reconfigurable CPW-to-slotline transitions, is designed to have a characteristic impedance of 50 ohm over the frequency band of concern. The slotline impedance, on the other hand, is around 90 ohm, which corresponds to a width of 0.2 mm in the design. The open-circuited radial stub of the first-order CPW-to-slotline transition has a radius of 19.6 mm and a flared angle of 60°, and a blocking capacitor and thin slits are added to the input CPW line and the far end of the radial open stub, respectively, to provide the necessary dc isolations.

To achieve pattern reconfigurability, as shown in Fig. 1(c), two PIN diodes are placed over the inputs of the open-circuited radial stub of the transitions, whereas the other two diodes are placed across the coupled slotlines of the CPW input. Based on the dc bias arrangement of PIN diodes, the proposed antenna can be fed by one of the three feeding configurations, which are referred to as the CPW feeding mode, the right-hand slot (RS) feeding mode, and the left-hand slot (LS) feeding mode. In this design the PIN diode selected is a MACOM MA4AGBPL912 AlGaAs beam lead PIN diode with a forward bias resistance of 4 ohm and reverse bias total capacitance of less than 0.022 pF at 10 GHz [17]. The dimension of the diode including the pins is about 0.63 by 0.18 mm^2. The diodes were attached to the CPW-to-slotline transitions by silver paste with the help of an optical microscope and hot pad. The dc bias voltage V_{DD} is either 3.3 V or -3.3 V on each side of the transition, and may be selected alternatively by a standard single-pole double-throw

TABLE I
BIAS CONDITIONS FOR THE RECONFIGURABLE ANTENNA

	Switches		PIN diodes			
	S₁	**S₂**	**D₁**	**D₂**	**D₃**	**D₄**
CPW feeding	V_{DD}	V_{DD}	ON	OFF	OFF	ON
Left slot feeding	V_{DD}	$-V_{DD}$	ON	OFF	ON	OFF
Right slot feeding	$-V_{DD}$	V_{DD}	OFF	ON	OFF	ON

(SPDT) switch. The current-limited resistors R_1 to R_4 are 560 ohm, and the diode current I_D is given by

$$I_D = \frac{V_{DD} - V_D}{R_1} = 3.5\ \mathrm{mA}. \quad (1)$$

In (1), V_D is the voltage across the diode, which is approximate to 1.35 V for $I_D = 10\ \mathrm{mA}$.

The reconfigurable transitions are then followed by another section of CPW line which is terminated by a pair of tapered slotlines. The tapered profile of the slotlines is described by the equations of a Vivaldi antenna [18]

$$y = c_1 e^{Rx} + c_2 \quad (2)$$

where

$$c_1 = \frac{y_2 - y_1}{e^{Rx_2} - e^{Rx_1}} \quad (3)$$

$$c_2 = \frac{y_1 e^{Rx_2} - y_2 e^{Rx_1}}{e^{Rx_2} - e^{Rx_1}}. \quad (4)$$

Here, $R = 0.15$ is the opening rate, $P_1 = (x_1, y_1)$ represents the start point, and $P_2 = (x_2, y_2)$ is the end point of the tapered profile. The initial width of the tapered slotline is 0.2 mm, i.e., a slotline impedance of 90 ohm. As the width of the slotline becomes wider, the line impedance rises accordingly and hence facilitates the radiations from the tapered slotline to free space with an intrinsic impedance of 377 Ohm. It is interesting to note that aside from the reconfigurable CPW-to-slotline transition, this antenna is in essence a wideband CPW-fed slotted bow-tie antenna with fairly omnidirectional xz-plane radiation patterns in most of the frequency band of interest.

Table I summarizes the dc biased configurations for the three antenna feeding schemes. When the antenna is intended to be operated in the CPW feeding mode, the diodes D_1, D_4 are turned on whereas D_2, D_3 are turned off. In this configuration, the wave injected into the CPW input line propagates directly downward to the radiating tapered slotlines. The two CPW-to-slotline transitions, on the other hand, are disabled by PIN diodes and have no function. Accordingly, the antenna simply behaves like a slotted bow-tie with the maximum radiation occurred in the broadside direction, i.e., along the z-axis.

For the antenna to be excited by the right-hand (RS) slotline, the diodes D_2, D_4 are kept forward biased whereas D_1, D_3 are reverse biased. Likewise, as the left-hand (LS) slotline is used as the feeding input, the diodes D_2, D_4 are turned off whereas D_1, D_3 are enabled. In either RS or LS feeding scheme, the unbalanced signal injected to the CPW input line will be transformed into a balanced slotline mode by one of the CPW-to-slotline transition upon the diode operation state. Accordingly, when operated in the RS or LS mode, the proposed antenna behaves more like a tapered slot antenna which demonstrates end-fire radiation patterns to either positive or negative x- axis with good front-to-back ratio.

It is worthwhile to mention that in designing the proposed reconfigurable antenna, tradeoffs occur between the impedance bandwidth and optimal radiation characteristics of the antenna. To accomplish widest operation bandwidth of the CPW-to-slotline transition, the slotline impedance should be selected as close to the impedance of the CPW line as possible, say, around 70 to 80 ohm. Nevertheless, a low-impedance slotline requires a narrow slot, for example, $G = 0.1\ \mathrm{mm}$ for the current design. Apart from the fabrication tolerance, a narrower slotline will in turn imply a narrower signal trace, i.e., S, for a given characteristic impedance of the CPW line. It therefore suggests that in the proposed design the two adjacent slotlines are geometrically in close proximity to each other, and are hence prone to give rise to parasitic couplings in either CPW (even) or coupled slotline (odd) mode. Such unwanted couplings will inevitably propagate downward to the inactive Vivaldi slot and may therefore diminish the high front-to-back ratio in either RS or LS operating mode. In addition, it is also noted that the parasitic radiations from the aperture of the radial open-circuited stub also impose a tradeoff between the optimal antenna impedance bandwidth and the desired reconfigurable radiation characteristics.

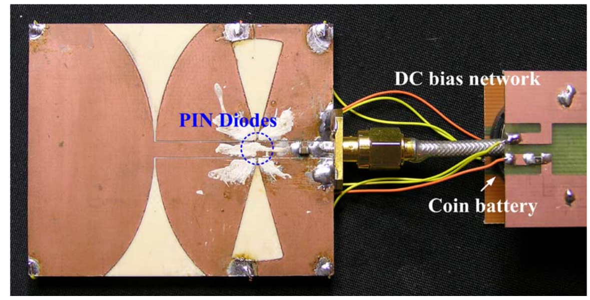

Fig. 2. Photograph of the proposed reconfigurable antenna.

III. SIMULATION AND MEASUREMENT RESULTS

The proposed antenna was first simulated by the EM full-wave simulator HFSS version 9.2 and then fabricated on a RO4003 substrate with a dielectric constant of 3.38 and thickness of 60 mil. The loss tangent of the substrate is 0.0027. The optimized parameters in accordance with the design considerations in Section II are given as follows: $L_1 = 25\ \mathrm{mm}$, $L_2 = 20\ \mathrm{mm}$, $L_3 = 15\ \mathrm{mm}$, $L_4 = 19.6\ \mathrm{mm}$, $L_5 = 15\ \mathrm{mm}$, $L_6 = 24.8\ \mathrm{mm}$, $S = 3\ \mathrm{mm}$, $G = 0.2\ \mathrm{mm}$, $W_1 = 23.3\ \mathrm{mm}$, $W_2 = 2\ \mathrm{mm}$, $W_3 = 21.5\ \mathrm{mm}$, and $a = 60^\circ$. The overall dimension of the proposed design, i.e., $L \times W$, is 60 by 50 mm^2. For demonstration purpose, the single-pole double-throw switches are not included in the design and the dc bias is provided by a pair of coin cell batteries. A photograph of the propose antenna along with the bias network and the connecting cable is shown in Fig. 2. The simulated and measured return

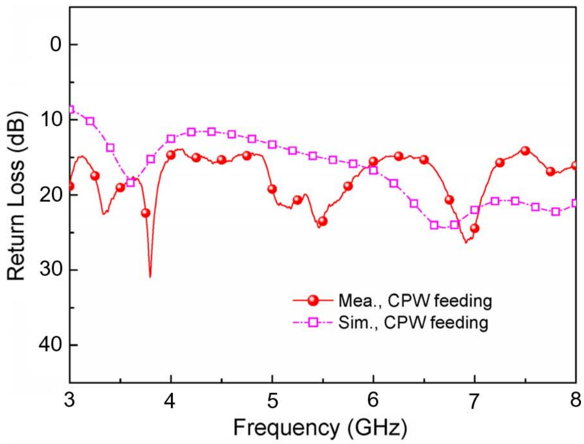

(a)

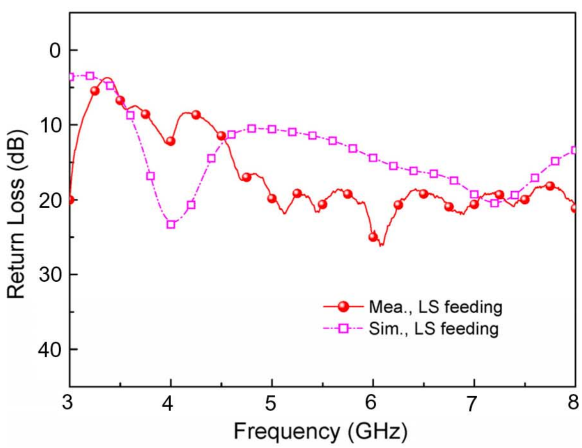

(b)

Fig. 3. Simulated and measured return losses. (a) CPW feeding. (b) LS feeding.

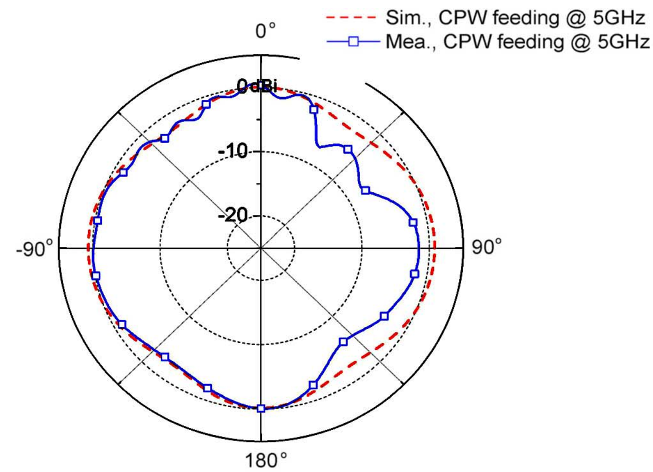

(a)

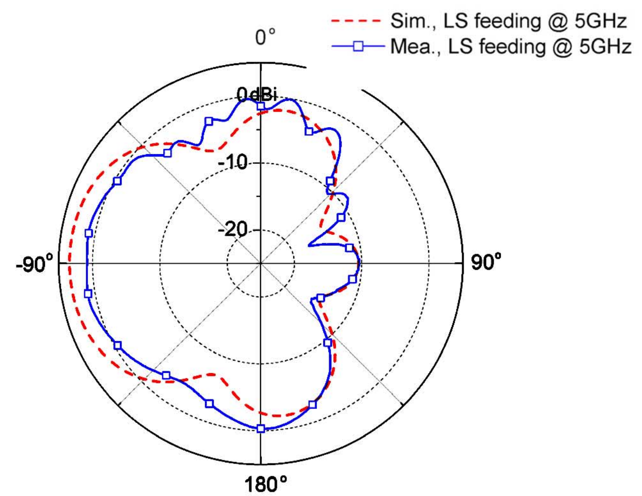

(b)

Fig. 4. Simulated and measured xz-plane radiation patterns at 5 GHz. (a) CPW feeding. (b) LS feeding.

losses of the proposed antenna operated in the CPW and LS feeding schemes are illustrated in Fig. 3(a) and (b), respectively. The measurement was taken by an Agilent E8362B network analyzer. It is shown in the figure that when the antenna is driven by the CPW feeding mode the impedance bandwidth with return loss better than 10 dB covers a very wide frequency range from 3 GHz to more than 8 GHz. As for the LS feeding mode, the antenna return loss exhibits slight deterioration for frequencies lower than 3.5 GHz but otherwise remains better than 10 dB. It should be emphasized that the actual antenna impedance bandwidth, which is from 3 GHz to more than 10 GHz, is by far wider than that shown in Fig. 3. Nevertheless, the reconfigurability of the proposed antenna becomes deteriorated for frequencies higher than 6.5 GHz, and is therefore less attractive for the present design. Accordingly, it is not shown here for the sake of simplicity.

The simulated and measured radiation patterns of the proposed antenna operated in the CPW and LS modes at 5 GHz in the xz-plane are shown in Fig. 4(a) and (b), respectively. In the simulation the reverse-biased diode was modeled by a perfect open circuit since the reverse-biased capacitance of the diode is relatively small at the frequency band of interest. On the other hand, instead of modeling the forward biased diode by a perfect short circuit [10], in our simulation the PIN diode was modeled by a constant current source of 3.5 mA with zero internal resistance. It is believed to be a better approximation to the actual operating condition in the measurement. The radiation patterns of the proposed antenna were measured in a $7 \times 3.2 \times 3\ \mathrm{m}^3$ anechoic chamber in National Taiwan University of Science and Technology. The measurement was performed by an Agilent E8362B network analyzer along with the NSI 2000 far-field measurement software. An EMCO 3115 double-ridged horn antenna was served as the standard antenna, and the distance between the transmitting and receiving antennas was 3.6 m. In the measurement the connecting cables were shielded by the absorbers to reduce the multipath interference. As shown in the figure, the agreement between the simulation and measurement is fairly well, and the slight discrepancy can be attributed to the fabrication tolerance, the interference from the dc bias lines and connecting cables, as well as from the lossless diode model used in the simulation. The simulated antenna peak gain is a little bit higher than the measure one, which is also likely a result of the lossless diode model. Moreover, referring to Fig. 4(a) and (b), it is noted that the antenna radiation pattern in the CPW mode is fairly omnidirectional, whereas the front-to-back ratio of the antenna in the LS feeding configuration is better than 11 dB. It preliminarily demonstrates the effectiveness of our proposed pattern reconfigurable antenna scheme. Similar results can be

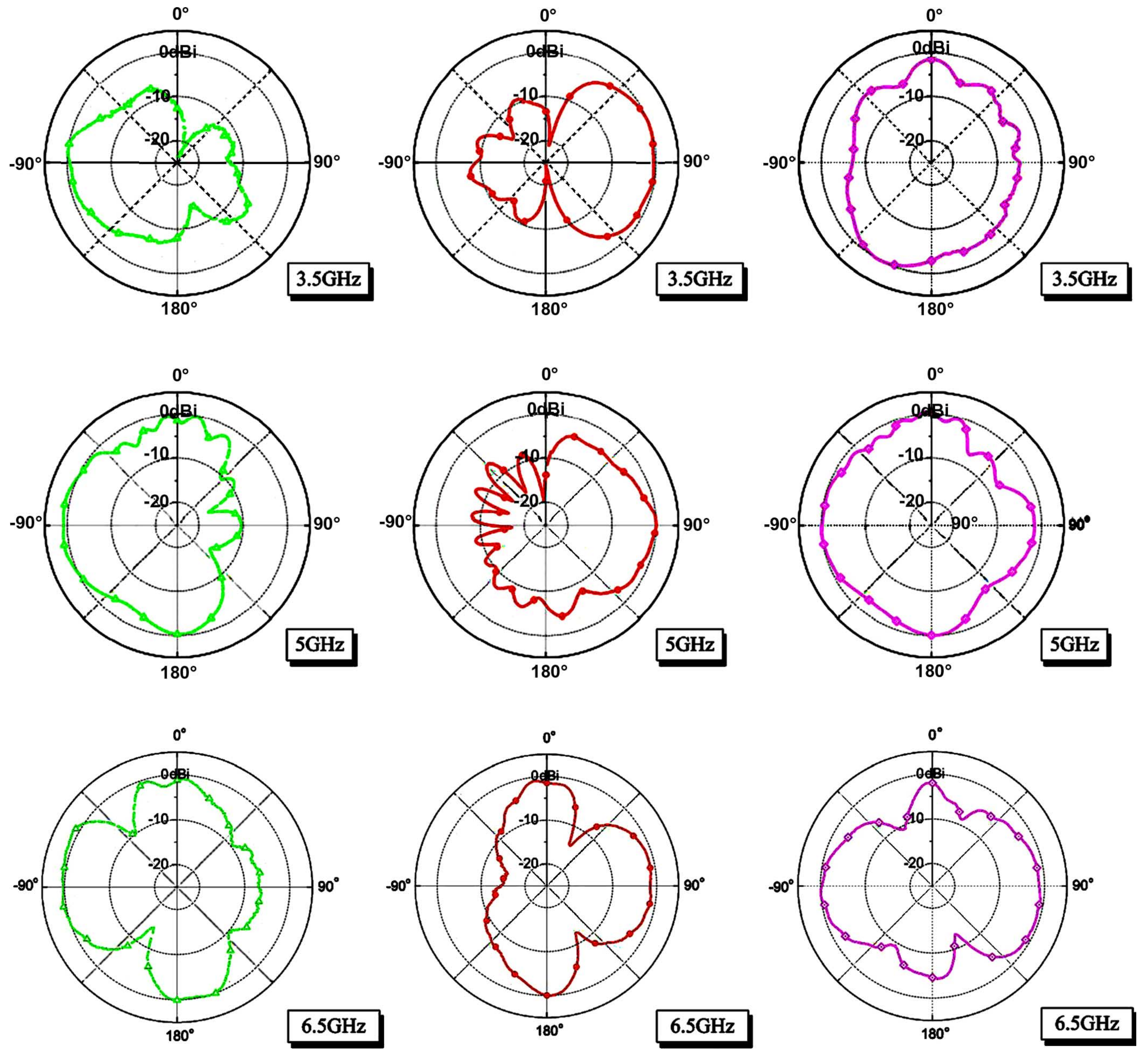

Fig. 5. Comparisons of the measured xz-plane antenna radiation patterns in LS, RS, and CPW feeding scheme at 3.5, 5, and 6.5 GHz. (–△–: co-polarization with LS feeding; –●–: co-polarization with RS feeding; –◇–: co-polarization with CPW feeding).

readily observed in the RS feeding mode but not shown here for simplicity.

To further manifest the reconfigurability of the proposed design, the measured antenna radiation patterns in the xz- and xy-planes for all three feeding configurations are illustrated in Figs. 5 and 6, respectively. The measured operating frequencies are the center frequency of the antenna, 5 GHz, and the frequencies at the band edges, i.e., 3.5 and 6.5 GHz. According to the figures, as the antenna is operated in the LS or RS mode, end-fire radiation patterns with the front-to-back ratio, for some angles better than 10 dB, can be readily observed in both principal plane-cuts throughout the frequency band of interest. The measured radiation patterns at 4 and 6 GHz also exhibit similar performance but are not shown here due to the limited space. Meanwhile, in the CPW feeding scheme the radiation patterns remain roughly a donut-like shape in most of the operating band with the axis of the donut pointing to the y-axis. Referring to Fig. 5, in the CPW mode the xz-plane radiation pattern possesses broadside-radiation characteristics at the lower frequency edge. It remains fairly omnidirectional in most of the band but begins to deteriorate for frequencies higher than 6 GHz. Although not shown here for simplicity, it is observed that the antenna eventually radiates bidirectionally toward the $\pm$x-axis for frequencies higher than 7 GHz. On the contrary, the xy-plane radiation patterns in the CPW feeding configuration, as illustrated in Fig. 6, consistently demonstrates butterfly-like shapes over the entire band.

In addition to the radiation patterns, the antenna transfer functions are reported to be helpful in providing a comprehensive understanding of the wideband antenna radiation characteristics

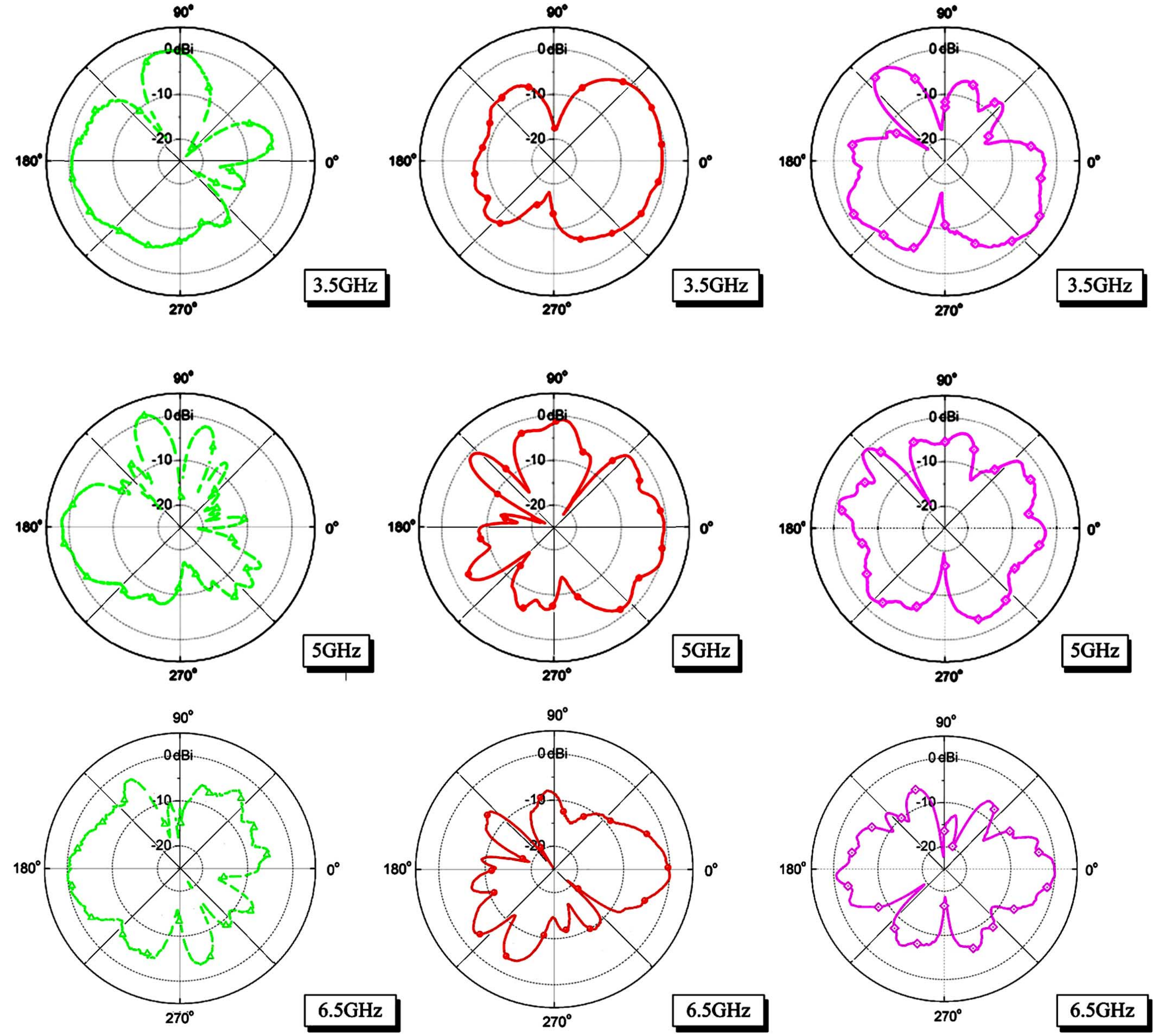

Fig. 6. Comparisons of the measured xy-plane antenna radiation patterns in LS, RS, and CPW feeding scheme at 3.5, 5, and 6.5 GHz. (−△−: co-polarization with LS feeding;: −●−: co-polarization with RS feeding; −◇−: co-polarization with CPW feeding).

over frequencies [19], [20]. In this work the proposed antenna is further examined by means of the gain responses versus frequencies at four specific reception angles. Fig. 7(a) to (d) illustrates the gain responses in the xz-plane at $\theta = 0^\circ$, 90°, 180°, and -90° over the frequency band of concern. Here only the radiation characteristics in the xz-plane for the RS and LS feeding configurations are discussed for the sake of simplicity. Referring to Fig. 7(b) and (d), the dramatic change of gain responses as the antenna being switched between RS and LS feeding schemes further demonstrates the pattern reconfigurability of the proposed design. The gain difference between the two end-fire radiation states is at least 10 dB and can be more than 20 dB around the center frequency of the operation band. For frequencies higher than 7 GHz, however, the end-fire radiation characteristics become less evident. Such performance degradation is most likely a result of the parasitic radiations from the open-circuited radial stub of the CPW-to-slotline transitions as well as from the parasitic coupling between the active and inactive slotlines, which have been discussed in the previous section. In addition, the antenna gain responses in the RS and LS feeding modes reveal very good agreement at $\theta = 180^\circ$ but somewhat discrepancy at $\theta = 0^\circ$. Such discrepancy can be mostly attributed to the fabrication tolerance of the antenna. The coupling from the connecting cable is also believed to have some contribution. Despite those nonideal effects during the fabrication and measurement, the gain responses in Fig. 7 further sustain the consistency of the wideband pattern reconfigurability of the proposed design.

IV. Conclusion

A new slotted bow-tie antenna with a pair of reconfigurable CPW-to-slotline transitions has been proposed and

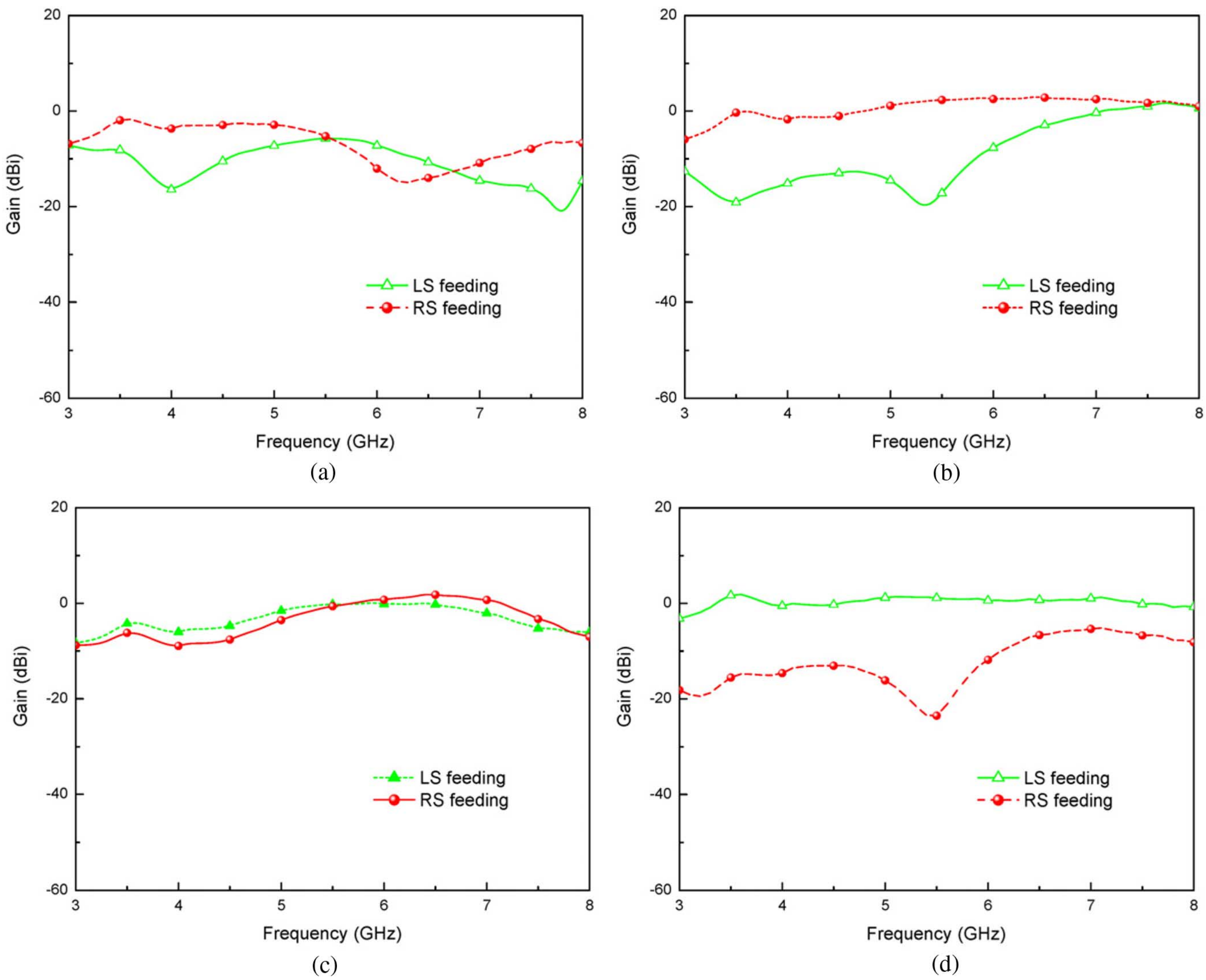

Fig. 7. Comparisons of the gain responses of the proposed antenna operated in the RS and LS feeding schemes at (a) $\theta = 0^\circ$, (b) $\theta = 90^\circ$, (c) $\theta = 180^\circ$, (d) $\theta = -90^\circ$ in the xz-plane.

demonstrated for pattern reconfigurability. By means of four PIN diodes and the associated dc bias network, it has been shown that the antenna has the ability to alternatively switch its radiation pattern between three states, i.e., a broadside radiation state with roughly omnidirectional pattern, and two end-fire radiation ones whose mainbeams are directed to opposite directions. The radiation characteristics of the proposed antenna have been carefully investigated in terms of radiation patterns in the principal plane-cuts as well as the gain responses versus frequencies. The experiment results agree well with the simulation ones, which demonstrate that the proposed design exhibits excellent pattern reconfigurability over the frequency range from 3.5 to 6.5 GHz. The future work will be in further improving the antenna impedance matching and the associate radiation characteristics at the lower frequency edge as well as in designing a miniaturized wideband CPW-to-slotline transition so as to avoid the undesired parasitic radiations and therefore to improve the antenna responses in higher frequencies. This antenna may find applications in a variety of wireless communication systems which are plagued by multipath interference and urge for pattern diversity.

REFERENCES

[1] W. H. Weedon, W. J. Payne, and G. M. Rebeiz, "MEMS-switched reconfigurable antennas," in *IEEE AP-S Int. Symp. Dig*, Boston, MA, Jul. 2001, vol. 3, pp. 654–657.

[2] D. Peroulis, K. Sarabandi, and L. P. B. Katehi, "Design of reconfigurable slot antenna," *IEEE Trans. Antennas Propag.*, vol. 53, pp. 645–654, Feb. 2005.

[3] N. Behdad and K. Sarabandi, "Dual-band reconfigurable antenna with wide tenability range," *IEEE Trans. Antennas Propag.*, vol. 54, pp. 409–416, Feb. 2006.

[4] G. H. Huff, J. Feng, S. Zhang, G. Cung, and J. T. Bernhard, "Directional reconfigurable antennas on laptop computers: Simulation, measurement and evaluation of candidate integration positions," *IEEE Trans. Antennas Propag.*, vol. 52, pp. 3220–3227, Dec. 2004.

[5] C. Jung, M. Lee, G. P. Li, and F. De Flaviis, "Reconfigurable scan-beam single-arm spiral antenna integrated with RF-MEMS switches," *IEEE Trans. Antennas Propag.*, vol. 54, pp. 455–463, Feb. 2006.

[6] S. Zhang, G. H. Huff, J. Feng, and J. T. Bernhard, "A pattern reconfigurable microstrip parasitic array," *IEEE Trans. Antennas Propag.*, vol. 52, pp. 2773–2776, Oct. 2004.

[7] H. Aïssat, L. Cirio, M. Grzeskowiak, J.-M. Laheurte, and O. Picon, "Reconfigurable circularly polarized antenna for short-range communication systems," *IEEE Trans. Microw. Theory Tech.*, vol. 54, pp. 2856–2863, Jun. 2006.

[8] M. Boti, L. Dussopt, and J.-M. Laheurte, "Circularly polarised antenna with switchable polarisation sense," *Electron. Lett.*, vol. 36, no. 18, pp. 1518–1519, Aug. 2000.

[9] F. Yang and Y. Rahmat-Samii, "A reconfigurable patch antenna using switchable slots for circular polarization diversity," *IEEE Microw. Wireless Compon. Lett.*, vol. 12, pp. 96–98, Mar. 2002.

[10] S. Nikolaou, R. Bairavasubramanian, C. Lugo, Jr., I. Carrasquillo, D. C. Thompson, G. E. Ponchak, J. Papapolymerou, and M. M. Tentzris, "Pattern and frequency reconfigurable annular slot antenna using PIN diodes," *IEEE Trans. Antennas Propag.*, vol. 54, pp. 439–448, Feb. 2006.

[11] G. H. Huff, J. Feng, S. Zhang, and J. T. Bernhard, "A novel radiation pattern and frequency reconfigurable single turn square spiral microstrip antenna," *IEEE Microw. Wireless Compon. Lett.*, vol. 13, pp. 57–59, Feb. 2003.

[12] E. R. Brown, "RF-MEMS switches for reconfigurable integrated circuits," *IEEE Trans. Microw. Theory Tech.*, vol. 46, pp. 1868–1880, Nov. 1998.

[13] D. E. Anagnostou, G. Zheng, M. T. Chryssomallis, J. C. Lyke, G. E. Ponchak, J. Papapolymerou, and C. G. Christodoulou, "Design, fabrication, and measurement of an RF-MEMS-based self-similar reconfigurable antenna," *IEEE Trans. Antennas Propag.*, vol. 54, pp. 422–432, Feb. 2006.

[14] K. J. Vinoy, K. A. Jose, V. K. Varadan, and V. V. Varadan, "Hilbert curve fractal antennas with reconfigurable characteristics," in *IEEE MTT-S Int. Microw. Symp. Dig.*, Phoenix, AZ, May 2001, vol. 1, pp. 381–384.

[15] J. S. Petko and D. H. Werner, "Miniature reconfigurable three-dimensional fractal tree antennas," *IEEE Trans. Antennas Propag.*, vol. 52, pp. 1945–1956, Aug. 2004.

[16] S. C. Yen and T. H. Chu, "A beam-scanning and polarization-agile antenna array using mutually coupled oscillating doublers," *IEEE Trans. Antennas Propag.*, vol. 53, pp. 4051–4057, Dec. 2005.

[17] MACOM, Homepage [Online]. Available: http://www.macom.com/ DataSheets/ MA4AGBLP912.pdf

[18] J. Shin and D. H. Schaubert, "A parameter study of stripline-fed Vivaldi notch-antenna arrays," *IEEE Trans. Antennas Propag.*, vol. 47, pp. 879–886, May 1999.

[19] T. G. Ma and S. K. Jeng, "Planar miniature tapered-slot-fed annular slot antennas for ultrawide-band radios," *IEEE Trans. Antennas Propag.*, vol. 53, pp. 1194–1202, Mar. 2005.

[20] Z. N. Chen, X. H. Wu, N. Yang, and M. Y. W. Chia, "Considerations for source pulses and antennas in UWB radio systems," *IEEE Trans. Antennas Propag.*, vol. 52, pp. 1739–1748, Jul. 2004.

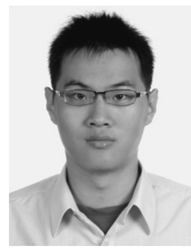

Sung-Jung Wu was born in Taipei, Taiwan, R.O.C., in 1980. He received the B.S. degree in electrical engineering from TamKang University (TKU), Taipei, R.O.C., in 2004, and the M.S. degree in electrical engineering from National Taiwan University of Science and Technology (NTUST), Taipei, R.O.C., in 2007. He is currently working toward the Ph.D. degree at National Chiao Tung University, Hsinchu, Taiwan, R.O.C.

From 2004 to 2005, he worked with the Foxconn Technology Co., Ltd., Taiwan, for the RF circuits in cdma2000 cellular phone. In 2007, he joined the Sunplus Technology Co., Hsinchu, where he is now a RF engineer. His research interests include mobile antenna designs, RFID tag antenna designs, and UWB antenna designs.

Tzyh-Ghuang Ma (S'00–M'06) was born in Taipei, Taiwan, R.O.C., in 1973. He received the B.S. and M.S. degrees in electrical engineering from National Taiwan University in 1995 and 1997, respectively, and the Ph.D. degree in Communication Engineering from National Taiwan University, Taipei, in 2005. From 1997 to 1999, he served in the Navy of the Republic of China as a second lieutenant. In 2005 he joined the faculty of the Department of Electrical Engineering, National Taiwan University of Science and Technology, where he is now an assistant Professor. His research interests include ultra-wideband antenna and RF front-end circuit designs, mobile antenna designs, radio frequency identification (RFID), and microwave passive circuit designs.